

Diffraction-limited I band imaging with faint reference stars

Robert N. Tubbs^a John E. Baldwin^b and Craig D. Mackay^a

^aInstitute of Astronomy, Cambridge University, Cambridge CB3 0HA, UK

^bCavendish Astrophysics Group, Cambridge University, Cambridge CB3 0HE, UK

ABSTRACT

The use of faint reference stars for the selection of good short exposure images has recently been demonstrated^{1,2} as a technique which can provide essentially diffraction-limited I band imaging from well-figured ground-based telescopes as large as 2.5 m diameter. The faint limiting magnitude and enhanced isoplanatic patch size for the selected exposures technique means that 20% of the night sky is within range of a suitable reference star for I-band imaging. Typically the 1%-10% of exposures with the highest Strehl ratios are selected. When these exposures are shifted and added together, field stars in the resulting images have Strehl ratios as high as 0.26 and FWHM as small as 90 milliarcseconds. Within the selected exposures the isoplanatic patch is found to be up to 50 arcseconds in diameter at 810 nm wavelength. Images within globular clusters and of multiple stars from the Nordic Optical Telescope using reference stars as faint as $I \sim 16$ are presented. The technique relies on a new generation of CCDs which provide sub-electron readout noise at very fast readout rates. The performance of the selection technique for various astronomical programs is discussed in comparison with natural guide star Adaptive Optics (AO).

Keywords: lucky exposures sky coverage diffraction limited visible CCD imaging adaptive optics

1. INTRODUCTION

In recent observations^{1,2} with the Nordic Optical Telescope we demonstrated that selection of the best images from a large dataset of short exposures can provide essentially diffraction-limited images at wavelengths shorter than $1 \mu\text{m}$ using ground-based telescopes as large as 2.5 m. The technique was shown to work reliably using reference stars as faint as $I = 15.9$, and even 30 arcseconds away from the reference star the FWHM of the image point-spread function was as small as 130 milliarcseconds (without the use of any deconvolution techniques).

The short exposure images were taken with an L3Vision CCD detector developed by E2V Technologies (formerly Marconi). These low-light level CCDs allow fast frame rate imaging with low readout noise.³ It is clear that they have significant signal to noise advantages over both conventional CCD systems and image-intensified photon-counting detectors. At low signal levels photon-counting⁴ with high quantum efficiency is possible even at fast readout rates.

This report describes the method we have used for frame selection, shifting and co-adding, and presents some preliminary results from the technique. All the images presented here were created from relatively short observations (2-10 minutes), but the potential of the technique to provide deep diffraction-limited images is clear.

Further author information: (Send correspondence to R.N.T.)

R.N.T.: E-mail: rnt20@cam.ac.uk, Telephone: +44 1223 337296

J.E.B.: E-mail: jeb@mrao.cam.ac.uk, Telephone: +44 1223 337299

C.D.M.: E-mail: cdm@ast.cam.ac.uk, Telephone: +44 1223 337543

2. BACKGROUND

Moments of near-perfect seeing at large optical telescopes have been discussed in the literature many times over a period of at least 60 years. One of the first detailed theoretical analyses of the frequency of these “lucky” instances of excellent image quality was published by Fried in 1978.⁵ He predicted that the probability of an exposure being essentially diffraction-limited (with Strehl ratio > 0.37) at a telescope of aperture diameter D for seeing defined by Fried’s⁶ parameter r_0 would be:

$$P \simeq 5.6 \exp\left(-0.1557(D/r_0)^2\right)$$

This probability is a strongly decreasing function of aperture diameter, so that care must be taken in choosing an appropriate aperture size. Hecquet and Coupinot⁷ showed that apertures of $4r_0 - 7r_0$ diameter are expected to provide the highest imaging resolution when selecting the best 1% of exposures. For I band observations under typical June/July seeing conditions conditions⁸ the 2.56 m diameter of the Nordic Optical Telescope corresponds to the upper end of this range, providing a good compromise between resolution and sensitivity.

Ideally the exposure times used should be short enough to freeze any atmospheric variations. Exposure times used for solar imaging are often sufficiently short, and image selection techniques have been used very successfully in this field for many years. High frame-rate CCD cameras have recently provided Mercury images^{9,10} with suitable exposure times, but observations of fainter astronomical targets have been limited to longer exposures due to signal-to-noise constraints. The image quality provided by exposure selection techniques gradually degrades as exposure times are increased until there is little improvement over local seeing conditions. Selected exposures with durations of 0.1s-4s have been very widely used for the imaging of fainter Solar System objects, but on only a small number of occasions has image selection been used for objects outside the Solar System (notable examples of image selection observations in galactic and extra-galactic astronomy can be seen in Refs: 11–16). Most of these studies have used image centroids for re-centring the selected exposures – numerical simulations indicate that re-centring exposures based upon the location of the brightest speckle gives a substantial improvement in the resulting resolution.

3. STREHL SELECTION TECHNIQUE

The image selection technique we have chosen for the analyses presented here utilises Strehl ratios calculated directly from images of unresolved reference stars within the field of view. The applicability of this technique to faint astronomical targets depends on the probability that a sufficiently bright reference star can be found within the isoplanatic patch prevailing at the times of the selected exposures. The intensity of the brightest speckle in the reference star image provides a measure of the image Strehl ratio, and the location of this speckle provides the tip-tilt correction for the shift and add procedure. The probability of finding a suitable natural reference star near an astronomical target is expected to be very much higher for the selected exposures technique than it is for natural guide star AO for a number of reasons:

1. The processes of image selection and image re-centring require a similar amount of light to that of tip-tilt correction (in the selected exposures a large fraction of the starlight falls in one speckle, improving the signal to noise for tip-tilt measurements). With our selected exposures technique the full light collecting power of a $\sim 7r_0$ telescope aperture is used, whereas AO wavefront sensors must perform tip-tilt correction using a sub-aperture of around $1r_0$ diameter.
2. AO systems use a feedback loop to correct wavefront errors, so the exposure times required in AO wavefront sensors are typically as short as $0.1t_0$. The selective exposures technique is passive so that an exposure time of t_0 is adequate (where t_0 is the atmospheric coherence time).
3. At the times when the selected exposures are acquired, the wavefronts entering the telescope are flat to within ~ 1 radian rms after tip-tilt correction. Using the relationship between r_0 and the variance of the wavefront phase across an aperture after tip-tilt correction¹⁷ it is possible to calculate an instantaneous value of r_0 appropriate for the selected exposures, which will have a value substantially larger than

the mean r_0 for the local seeing conditions. The improved wavefront flatness is expected to provide a substantial improvement in the isoplanatic patch size for the technique as compared to conventional speckle imaging techniques. For the best 0.3% of exposures selected at a telescope of diameter $7r_0$ the isoplanatic patch should be doubled in size. The enhancement to the isoplanatic patch size may not be as pronounced at rare instances when improved wavefront flatness is brought about by two phase screens widely separated in the atmosphere cancelling each other out.

Points 1. and 2. above should theoretically lead to an improvement of around 6 magnitudes in the limiting magnitude of reference star which can be used for image selection, compared to the natural guide star AO case.

The fraction of exposures to be selected is decided during post processing of the data. The selection criteria used determines the sensitivity, image resolution and isoplanatic patch size, and can be tailored to the needs of the investigator.

4. LOW LIGHT LEVEL CCD (L3VISION)

In many previous high frame rate imaging observations, detector read-out noise has compromised the image quality and substantially reduced the limiting magnitude which can be obtained. The recent development of CCDs with negligible readout noise³ has eliminated the noise penalty for fast readout, providing an improvement in the limiting magnitude of reference star which can be used and allowing the detection of faint objects in the field.

The technology behind the L3Vision detectors is disclosed in Ref: 18. In essence a conventional CCD structure is used with the output register extended with an additional section that has one of the three phases clocked with a much higher voltage than is needed purely for charge transfer. The large electric fields that are established in the semiconductor material beneath pairs of serial transfer electrodes cause charge carriers to be accelerated to high velocities. Additional charge carriers can then be generated by impact ionisation. The charge multiplication per transfer is really quite small, typically one percent but with a large number of transfers (591 for the device used here) substantial electronic gains may be achieved. The output of this extended serial register is passed on to a conventional CCD output amplifier. The electronic noise of this amplifier is now divided by the gain factor of the multiplication register which, if this gain is high enough, will reduce the effective output read noise to levels much smaller than one electron rms. The gain register introduces additional noise to the device dominated by the statistics of the amplification process. This noise is proportional to the square-root of the signal level. At low signal levels and high multiplication register gain the readout noise is negligible and photon-counting can be performed.

5. OBSERVATIONS AND DATA REDUCTION

On 2001 July 6th we undertook high frame rate imaging observations at the Cassegrain focus of the 2.56 m Nordic Optical Telescope using a camera built around a low-noise L3Vision CCD. The camera comprised a front-illuminated 576×288 pixel frame-transfer CCD65 with $20 \times 30 \mu\text{m}$ pixels, cooled in a liquid nitrogen dewar to minimise the dark current. The CCD was run by an AstroCam 4100 controller modified to provide a variable voltage clock signal for the output gain register of the CCD. We used frame rates between 18 Hz and 140 Hz, with sub-array readout where necessary.

The f/11 beam at the focus was converted to f/60 using a single achromat, giving an image scale of 27×40 milliarcseconds per pixel and a total imaging area of 11.5×15.4 arcseconds. In order to investigate the image quality achieved at large angular separations from the reference star, the camera optics were designed so that light from two regions of the sky separated by 25 arcsec could be superimposed on the CCD. This allowed science targets to be imaged at separations of up to 30 arcseconds from the reference star. All the observations were made at 810 nm with a top-hat filter of 120 nm bandwidth and with no autoguider in operation.

Additional observations were taken for two hours on 2002 July 25th through severe Saharan dust extinction at the Nordic Optical Telescope, and again on 2002 July 26th through significantly clearer skies. It has not been possible to fully reduce any of the data from these runs, but two preliminary images based on runs of

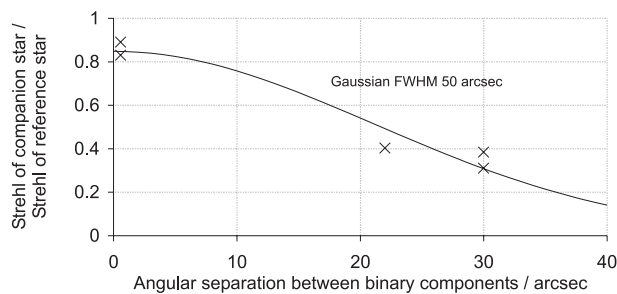


Figure 1. The isoplanatic patch for the selected exposures technique was investigated using binary star systems with a range of angular separations. One binary component was used as the reference star for image selection, shifting and co-adding. The Strehl ratio of the binary companion divided by the Strehl ratio for the reference star is plotted against the angular separation between the binary companions.

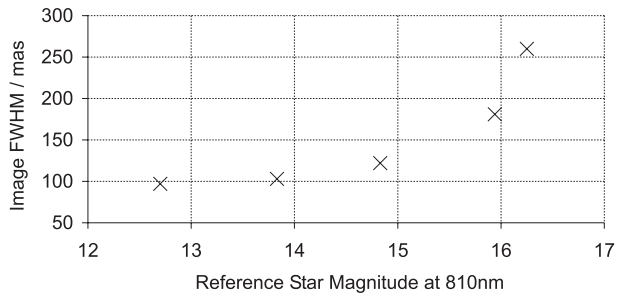


Figure 2. Dependence of image resolution on reference star magnitude for a range of reference stars in M13. Typical image FWHM are given in milliarcsec for stars within a few arcsec of the reference star, for a range of reference stars.

5-10 minutes observing time have been included (Figures 5 and 6, discussed in Section 6). The pixel scale for these observations was 25×37 milliarcseconds.

In order to convert the short exposure images taken on the rectangular pixel CCD array into square pixel arrays and to improve the sampling of the images, the individual short exposure images were resampled using sinc interpolation to give 4 times as many pixels in the x coordinate and 6 times as many pixels in the y coordinate.

The accuracy of measurement of the Strehl ratio and position of the brightest speckle was improved by convolving the individual frames with the diffraction-limited telescope point-spread function before these parameters were calculated. The peak intensity in the convolved images represents the location where correlation with the diffraction-limited point-spread function is maximised, providing a very good estimate for the location and intensity of a diffraction-limited speckle within the original image. After frames had been selected based on the Strehl ratio for the brightest speckle found, the corresponding unconvolved exposures were shifted and co-added to produce the final image.

6. RESULTS

The size of the isoplanatic patch in Strehl-selected exposures was deduced from observations of the binary stars HD 203991, 8 Lac and 61 Cygnii, which have separations of 0.6, 22 and 30 arcsec respectively. These were all bright enough that the selection and image shift correction for exposures was free of the effects of readout noise and small number statistics in photon detection. One component of each binary was used as the reference to select the best 1% of the exposures, for which both the image full width at half-maximum intensity (FWHM) and Strehl ratio of the other component were measured. Figure 1 shows the fractional reduction in Strehl ratio of the second component as a function of angular separation from the reference star. A Gaussian fit to the points gives 50 arcseconds for the FWHM of the isoplanatic patch for these selected frames, taken during a period in which the mean seeing was 0.51 arcsec. The image FWHM for objects 30 arcsec from the reference star using the best 1% from a run of 4000 exposures of 61 Cygnii was 130 milliarcsec, only slightly poorer than the FWHM of ~ 80 milliarcsec expected for a well sampled diffraction-limited point-spread function. The measured FWHM is increased to 230 milliarcsec when selecting the best 10% of exposures, and 300 milliarcsec when selecting all the exposures for a shift-and-add image.

The effect of reference star magnitude on the quality of the resulting image was studied using observations with the full field of view of the CCD in a densely populated region of M13 under 0.46 arcsecond I-band

seeing conditions (corresponding to 0.51 arcsecond seeing at 500 nm). The frame rate for these observations was limited to 18 Hz, allowing image motion to slightly blur the exposures. This limited the Strehl ratios for reconstructed images to ≤ 0.16 , with image FWHM of ~ 100 milliarcsec. Data was taken from 6 runs of 1000 frames each. The selection of the best 1% of the 6000 exposures worked successfully with reference stars as faint as $I = 15.9$. The effects of “over-resolution”¹⁶ on faint reference stars were avoided by using other objects in the field for image quality measurements. Figure 2 shows the variation in the image FWHM of nearby stars when a range of different stars are used as the reference for image selection, shifting and adding. I band stellar magnitudes were taken from Ref. 19. The Strehl ratios with reference stars of $I = 13.8$ and $I = 15.9$ are 0.13 and 0.065 respectively, a substantial improvement over the value of ~ 0.019 for conventional astronomical images generated by summing all of the exposures in a run without recentering the exposures.

It is clear from Figure 2 that the measurement of the Strehl ratio and position of the brightest speckle works well with reference stars as faint as $I = 15.9$ using our existing CCD camera. When combined with the large isoplanatic patch size demonstrated by Figure 1, this allows imaging over a very substantial fraction of the night sky – 8% of the South Galactic Pole region (based on 400 stars per square degree²⁰ with $I \leq 15.9$) and an average of 20% over the whole sky. In comparison, I band natural guide star adaptive optics is typically limited to $I \leq 10$ for high-order correction,²¹ with a significantly smaller isoplanatic patch and hence very much poorer sky coverage around suitable reference stars.

Figure 3a shows a small field in M13 around the bright star labelled *A* in Ref. 19. An $I = 12.7$ reference star was used for image selection and re-centring as shown in the Figure. Slight asymmetry in the faint halos around the stars may have resulted from poor charge transfer efficiency at low signal levels on the CCD – a result of the unusually low operating temperature. For this figure the best 10% of exposures were selected, giving typical stellar FWHM of ~ 120 milliarcseconds. This compares very favourably with the FWHM on HST WFPC2 images – typically 140 milliarcseconds on the PC chip and 190 milliarcseconds on the Wide Field CCDs. Cross sections through $I = 13.8$ and $I = 14.9$ stars are shown in Figure 3b.

The best 1% of exposures selected from this 5.5 minute observation of M13 using the same reference star gave an image with FWHM of < 0.1 arcseconds and showed stars as faint $I = 19$. For an hour of observing this limiting magnitude will be increased to at least $I = 21$.

In order to assess the image quality, the 60 best exposures of M13 were separated into two groups of 30. The exposures in each group were shifted and added together giving two independent images of the field in M13. These images were then convolved with the diffraction-limited telescope point-spread function. Measurements were made of the location and intensity of the brightest pixel for each star, providing crude relative astrometry and photometry within the images. The rms difference in astrometry between the two independent datasets was found to be 6 milliarcsec, and the rms difference in stellar magnitudes was 0.02. With longer observations the accuracy of the astrometry and photometry is expected to improve substantially, potentially allowing accurate measurements of globular cluster velocity dispersions and ground-based photometric variability studies.

Figure 4 shows a field near the centre of the globular cluster M15. The $I = 13.1$ star circled was used for exposure selection, shifting and co-adding. This image was generated by selecting the best 1% of exposures from 2000 frames taken at 18 Hz frame rate.

Figure 5 shows an image of a nearby field in M15 which has been contrast-enhanced to highlight some of the faintest stars. The location of the cluster centre as determined in Ref: 22 is marked with a cross. Over 70 stars brighter than $I = 19$ are visible in this 13×10 arcsecond region alone. This image was generated from the best 3% of exposures taken during 5 minutes of observing time at the NOT. The image FWHM are typically 240×140 milliarcseconds – although not diffraction-limited, this represents a substantial improvement over the 0.6 arcsecond conventional (seeing-limited) image. The reduction in resolution when compared with observations of M13 in July 2001 is largely attributable to the very strong dependence of the image FWHM in selected exposures on the local seeing conditions. For the observations of M13 the long exposure image FWHM and short exposure image Strehl ratios are consistent with an I-band r_0 size of 0.36 m, with the telescope aperture hence measuring $7.1r_0$ diameter (this I-band r_0 size would correspond to a 500 nm long-exposure seeing disk of 0.51 arcseconds FWHM). For the observations of M15, the r_0 size was 0.28 m, making the aperture diameter equal to $9.2r_0$. The image resolution obtained from selecting a few percent of exposures is

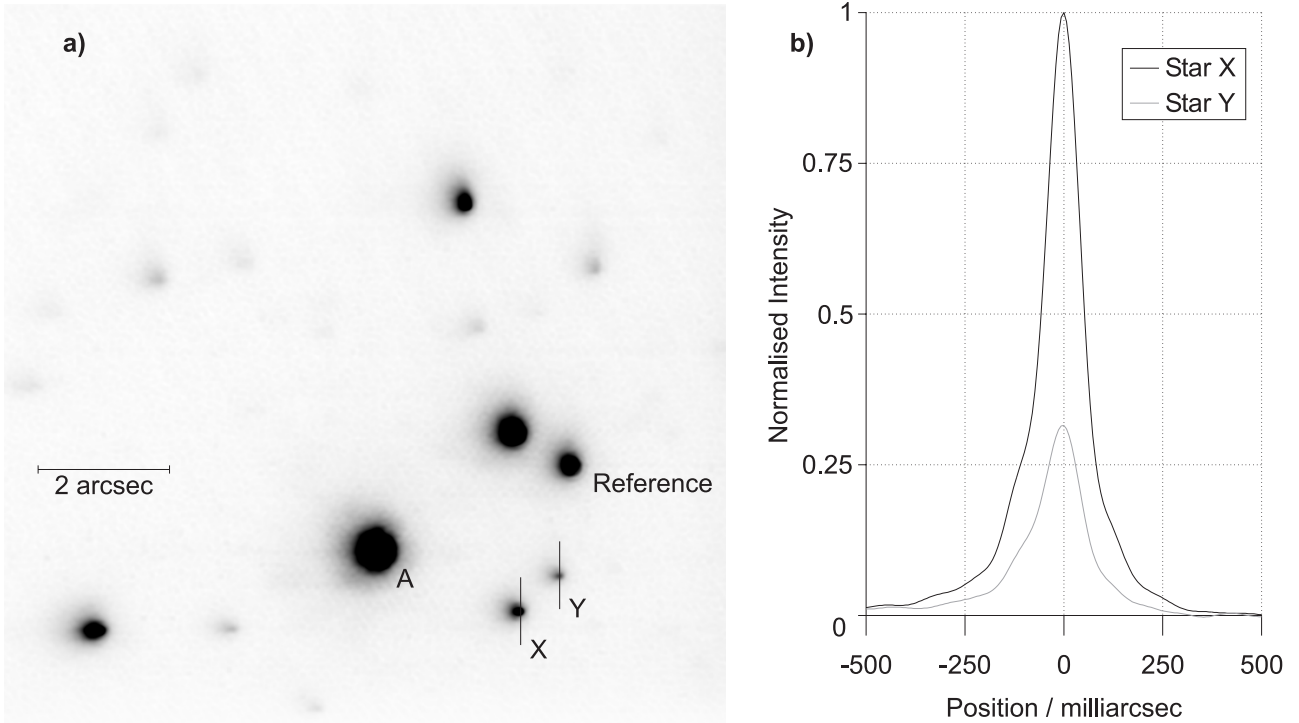


Figure 3. The best 10% of exposures from a field in M13 were selected, shifted and added to produce image **a**. The reference star for frame selection and recentring has been labelled. North is at the top. Cross-sections through the $I = 13.8$ and $I = 14.9$ stars labelled *X* and *Y* are shown in part **b**, with FWHM of ~ 120 milliarcseconds.

known to drop rapidly with aperture diameter for apertures greater than $\sim 7r_0$.⁷ With bright reference stars an improvement in resolution can be obtained by stopping down the telescope aperture, at the expense of a loss of sensitivity.

The 5 minute observation of the region shown in Figure 5 is the only data which has so far been analysed from the night of 2002 July 26th. Eight adjoining fields were also observed on that night and we eventually intend to form a mosaic from all of the data.

Figure 6 shows an image of the multiple star system Gliese 569, generated by selecting the best 4% of exposures from 10 minutes of observing time on 2002 July 25th. The faint companion visible in the inset image is thought to be a triple brown dwarf system.²³ The widest separation in the triple system is slightly larger than the diffraction limit of the NOT at 810nm, and under more typical June/July seeing conditions it should be possible to estimate an I-band magnitude difference for the two principle components.

Two short exposures taken from a run on a faint star are shown in Figure 7. Figure 7a shows a surface plot of the intensity in a selected exposure (one with high Strehl ratio), while Figure 7b shows the exposure with the median Strehl from the same run. The improvement in signal to noise for the shift-and-add process provided by exposure selection is apparent from the difference between the peak intensity in 7a and 7b. It is this signal to noise improvement allows the image selection technique to use fainter reference stars than those used for conventional shift-and-add.

7. FUTURE PROSPECTS OF EXPOSURE SELECTION

The exposure selection technique described here has the potential to provide diffraction-limited imaging from any medium sized ground-based telescope which has well-figured optics and good astronomical seeing conditions. For high-resolution observations the technique requires a telescope aperture which is no more than $7r_0$ diameter.

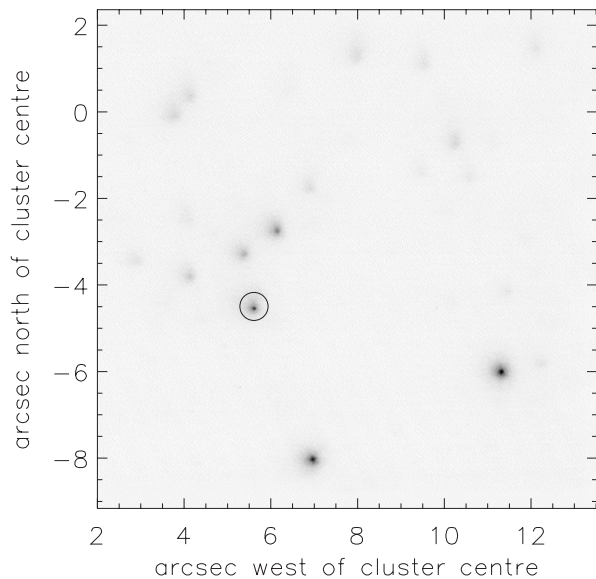


Figure 4. The best 1% of exposures from a field near the centre of M15 were selected, shifted and added to produce this image. The $I=13.1$ reference star used for frame selection and recentring has been circled. The exposures were selected from data taken during 2 minutes of observing time at the NOT. North is to the lower left.

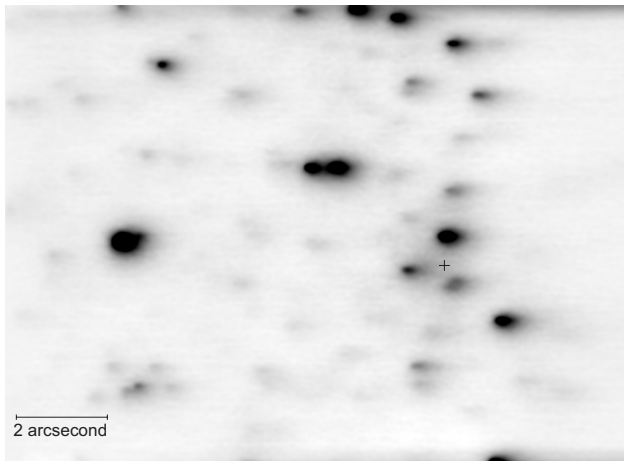


Figure 5. Contrast-enhanced image of a 13×10 arcsecond region around the core of M15. This image was generated from the best 3% of exposures taken during 5 minutes of observing time at the NOT. The location of the cluster centre is marked with a cross.

If the seeing conditions are 0.5 arcseconds at 500 nm, then $7r_0$ corresponds to a diameter of 2.9 m at 900 nm and 8.5 m at $2.2 \mu\text{m}$. Seeing conditions are known to vary during the night,²⁴ and if seeing degrades substantially then high resolution observations can only be performed after the telescope aperture has been stopped down.

The magnitude limit of this image selection technique will be improved by the development of thinned anti-reflection coated L3Vision CCDs. With such a device one could expect to detect $I \simeq 23$ unresolved sources in an hour of observing if the device was operated in photon counting mode at a 2.5 m telescope. This would allow scientifically rewarding studies such as the accurate measurement of velocity dispersions in globular clusters, and the potential for accurate ground-based photometry in crowded fields such as globular clusters and of small-separation gravitational lenses.

The rarity of “Lucky Exposures” means that image selection techniques are rather wasteful of starlight, making them unpopular with many telescope operators. However, the ability to perform I-band diffraction-limited imaging of fields of up to 50 arcseconds diameter using reference stars so faint that they are widely available across the whole night sky has enormous scientific potential for medium-sized ground-based telescopes. Natural guide star I-band adaptive optics systems are only capable of operating in the vicinity of relatively bright reference stars, and cannot compete with exposure selection for imaging the vast majority of astronomical sources.

The relatively low cost and ease of construction of high frame rate L3Vision cameras make them attractive propositions for a large number of medium-sized optical telescopes. The probability of obtaining a “lucky exposure” is substantially increased if the low-order wavefront aberrations are corrected, making this image selection technique applicable to larger telescopes which have AO systems optimised for wavefront correction at infra-red wavelengths (hence providing low-order correction in the visible). Further discussion of short-exposure image selection with AO systems can be found in Refs: 25–27.

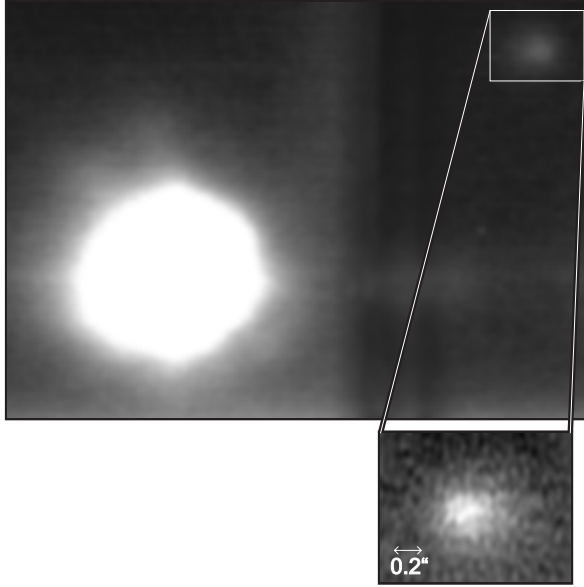


Figure 6. The best 4% of exposures of the multiple star system GJ 569. The faint object on the right is thought to be a brown dwarf triple system.²³ The images were selected from 10 minutes of observing time at the NOT, on a night with high Saharan dust extinction at the observatory and slightly below-average seeing conditions for July.

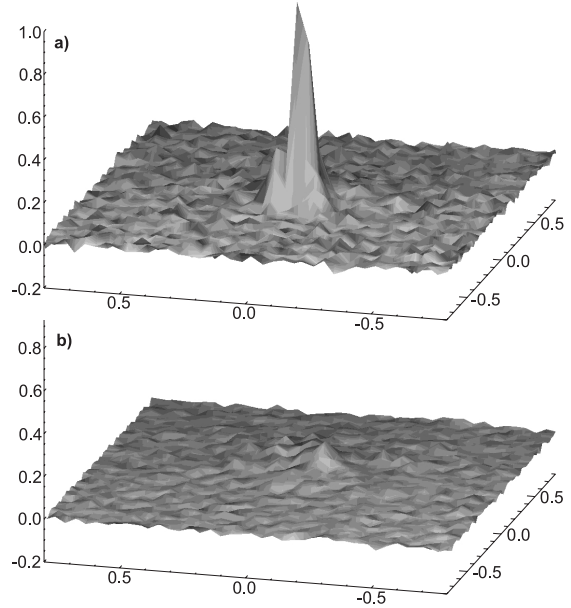


Figure 7. Surface plots of intensity in two example exposures taken from a run on a faint star. Plot **a)** shows an exposure with high Strehl ratio, while plot **b)** shows the exposure with the median Strehl ratio from the same run. The improvement in signal to noise for the shift-and-add process provided by exposure selection is apparent from the difference between the peak intensity in **a)** and **b)**.

8. CONCLUSIONS

The exposure selection technique described here has the potential to provide diffraction-limited imaging from any medium sized ground-based telescope which has well-figured optics and good astronomical seeing conditions. The technique works well over a larger isoplanatic patch than is accessible to adaptive optics, and can utilise reference stars which are much fainter than those required for adaptive optics.

With I-band observations at the 2.56 m Nordic Optical Telescope we have demonstrated that the image selection technique can provide near diffraction-limited I-band imaging over 20% of the night sky using low light level detectors recently developed by E2V Technologies. Fields as large as 50 arcseconds in diameter around a reference star can be imaged at high-resolution, and the use of reference stars as faint as $I \sim 15.9$ has been demonstrated. The development of thinned anti-reflection coated L3Vision CCDs will improve the reference star magnitude limit to fainter than $I = 16$ and allow the detection of sources in the field as faint as $I \sim 23$ in an hour of observation.

ACKNOWLEDGMENTS

The Nordic Optical Telescope is operated on the island of La Palma jointly by Denmark, Finland, Iceland, Norway and Sweden, in the Spanish Observatorio del Roque de los Muchachos of the Instituto de Astrofísica de Canarias.

This project has been supported by the European Commission through the *Access to Research Infrastructures Action of the Improving Human Potential Programme*, awarded to the Instituto de Astrofísica de Canarias to fund European Astronomers' access to the European Northern Observatory, in the Canary Islands.

REFERENCES

1. R. N. Tubbs, J. E. Baldwin, C. D. Mackay, and G. C. Cox, "Diffraction-limited CCD imaging with faint reference stars," *A&A* **387**, pp. L21–L24, May 2002.
2. J. E. Baldwin, R. N. Tubbs, G. C. Cox, C. D. Mackay, R. W. Wilson, and M. I. Andersen, "Diffraction-limited 800 nm imaging with the 2.56 m Nordic Optical Telescope," *A&A* **368**, pp. L1–L4, Mar. 2001.
3. C. D. Mackay, R. N. Tubbs, R. Bell, D. J. Burt, P. Jerram, and I. Moody, "Subelectron read noise at MHz pixel rates," in *Proc. SPIE*, **4306**, pp. 289–298, May 2001.
4. P. Jerram, P. J. Pool, R. Bell, D. J. Burt, S. Bowring, S. Spencer, M. Hazelwood, I. Moody, N. Catlett, and P. S. Heyes, "The LLCCD: low-light imaging without the need for an intensifier," in *Proc. SPIE*, **4306**, pp. 178–186, May 2001.
5. D. L. Fried, "Probability of getting a lucky short-exposure image through turbulence," *Optical Society of America Journal* **68**, pp. 1651–1658, Dec. 1978.
6. D. L. Fried, "Optical Resolution Through a Randomly Inhomogeneous Medium for Very Long and Very Short Exposures," *Optical Society of America Journal* **56**, pp. 1372–1379, 1966.
7. J. Hecquet and G. Coupinot, "A gain in resolution by the superposition of selected recentered short exposures," *Journal of Optics* **16**, pp. 21–26, Feb. 1985.
8. C. Munoz-Tunon, J. Vernin, and A. M. Varela, "Night-time image quality at Roque de LOS Muchachos Observatory," *Astronomy and Astrophysics Supplement Series* **125**, pp. 183–193, Oct. 1997.
9. R. F. Dantowitz, S. W. Teare, and M. J. Kozubal, "Ground-based high-resolution imaging of mercury," *AJ* **119**, pp. 2455–2457, May 2000.
10. J. Baumgardner, M. Mendillo, and J. K. Wilson, "A Digital High-Definition Imaging System for Spectral Studies of Extended Planetary Atmospheres. I. Initial Results in White Light Showing Features on the Hemisphere of Mercury Unimaged by Mariner 10," *AJ* **119**, pp. 2458–2464, May 2000.
11. J.-L. Nieto, A. Llebaria, and S. di Serego Alighieri, "Photon-counting detectors in time-resolved imaging mode - Image recentering and selection algorithms," *A&A* **178**, pp. 301–306, May 1987.
12. J.-L. Nieto, S. Roques, A. Llebaria, C. Vanderriest, G. Lelievre, S. di Serego Alighieri, F. D. Macchetto, and M. A. C. Perryman, "High-resolution imaging of the double QSO 2345 + 007 - Evidence for subcomponents," *ApJ* **325**, pp. 644–650, Feb. 1988.
13. G. Lelievre, J.-L. Nieto, E. Thouvenot, D. Salmon, and A. Llebaria, "Very high resolution imaging using sub-pupil apertures, recentering and selection of short exposures," *A&A* **200**, pp. 301–311, July 1988.
14. D. Crampton, R. D. McClure, J. M. Fletcher, and J. B. Hutchings, "A search for closely spaced gravitational lenses," *Astronomical Journal* **98**, pp. 1188–1194, Oct. 1989.
15. J.-L. Nieto, M. Auriere, J. Sebag, J. Arnaud, G. Lelievre, A. Blazit, R. Foy, S. Bonaldo, and E. Thouvenot, "The optical counterpart of the X-ray binary in the globular cluster NGC 6712," *A&A* **239**, pp. 155–162, Nov. 1990.
16. J.-L. Nieto and E. Thouvenot, "Recentering and selection of short-exposure images with photon-counting detectors. I - Reliability tests," *A&A* **241**, pp. 663–672, Jan. 1991.
17. R. J. Noll, "Zernike polynomials and atmospheric turbulence," *Optical Society of America Journal* **66**, pp. 207–211, Mar. 1976.
18. D. Burt and R. Bell, "CCD imagers with multiplication register," *European Patent Application Bulletin* **39**, p. EP 0 866 501 A1, Sept. 1998.
19. R. L. Cohen, P. Guhathakurta, B. Yanny, D. P. Schneider, and J. N. Bahcall, "Globular Cluster Photometry with the Hubble Space Telescope. VI. WF/PC-I Observations of the Stellar Populations in the Core of M13 (NGC 6205)," *AJ* **113**, pp. 669–681, Feb. 1997.
20. N. Reid and G. Gilmore, "New light on faint stars. II - A photometric study of the low luminosity main sequence," *MNRAS* **201**, pp. 73–94, Oct. 1982.

21. J. E. Graves, M. J. Northcott, F. J. Roddier, C. A. Roddier, and L. M. Close, "First light for hokupa'a: 36-element curvature ao system at uh," *SPIE Proceedings* **3353**, pp. 34–43, Sept. 1998.
22. P. Guhathakurta, B. Yanny, D. P. Schneider, and J. N. Bahcall, "Globular Cluster Photometry With the Hubble Space Telescope. V. WFPC Study of M15's Central density Cusp," *Astronomical Journal* **111**, pp. 267–+, Jan. 1996.
23. M. Kenworthy, K. Hofmann, L. Close, P. Hinz, E. Mamajek, D. Schertl, G. Weigelt, R. Angel, Y. Y. Balega, J. Hinz, and G. Rieke, "Gliese 569B: A Young Multiple Brown Dwarf System?," *ApJL* **554**, pp. L67–LL70, June 2001.
24. R. Racine, "Temporal Fluctuations of Atmospheric Seeing," *Publications of the Astronomical Society of the Pacific* **108**, pp. 372–+, Apr. 1996.
25. C. D. Mackay, J. E. Baldwin, and R. N. Tubbs, "Noise free detectors in the visible and infrared: Implications for the design of next-generation ao systems and large telescopes," in *Proc. SPIE*, **4840**, p. (in press), Aug. 2002.
26. M. C. Roggemann, C. A. Stoudt, and B. M. Welsh, "Image-spectrum signal-to-noise-ratio improvements by statistical frame selection for adaptive-optics imaging through atmospheric turbulence," *Optical Engineering* **33**, pp. 3254–3264, Oct. 1994.
27. S. D. Ford, M. C. Roggemann, and B. M. Welsh, "Frame selection performance limits for statistical image reconstruction of adaptive optics compensated images," in *Proc. SPIE Vol. 2534, p. 235-246, Adaptive Optical Systems and Applications, Robert K. Tyson; Robert Q. Fugate; Eds.*, **2534**, pp. 235–246, Aug. 1995.